

Ultra-shallow quantum dots in an undoped GaAs/AlGaAs 2DEG

W. Y. Mak,¹ F. Sfigakis,^{1, a)} K. Das Gupta,^{1,2} O. Klochan,³ H. E. Beere,¹ I. Farrer,¹ J. P. Griffiths,¹ G. A. C. Jones,¹ A. R. Hamilton,³ and D. A. Ritchie¹

¹⁾ Cavendish Laboratory, University of Cambridge, Cambridge, United Kingdom

²⁾ Department of Physics, Indian Institute of Technology, Mumbai, India

³⁾ School of Physics, University of New South Wales, Sydney, Australia

We report quantum dots fabricated on very shallow 2-dimensional electron gases (2DEG), only 30 nm below the surface, in undoped GaAs/AlGaAs heterostructures grown by molecular beam epitaxy. Due to the absence of dopants, an improvement of up to two orders of magnitude in mobility with respect to doped heterostructures with similar depths is observed. These undoped wafers can easily be gated with surface metallic gates patterned by e-beam lithography, as demonstrated here from single-level transport through a quantum dot showing large charging energies (up to 1.75 meV) and excited state energies (up to 0.5 meV).

Modulation doping in molecular beam epitaxy (MBE) growth has been an extremely successful technique in reducing scattering from ionized dopants by separating the two-dimensional electron gas (2DEG) from the (intentional) dopants by an undoped “spacer” layer.¹ With this technique (among others²), record high mobilities of up to $36 \times 10^6 \text{ cm}^2/\text{Vs}$ at an electron carrier density of $3 \times 10^{11} \text{ cm}^{-2}$, equivalent to a scattering length exceeding 0.3 mm, have been achieved in GaAs/AlGaAs heterostructures.³ However, the typical 2DEG depths of such high-mobility heterostructures (300–600 nm) makes them unsuitable for devices with sub-micron surface gates defined by e-beam lithography. Indeed, large distances between the 2DEG and gates smear the electrostatic potential pattern transferred electrostatically to the 2DEG, resulting in a weak confinement potential in mesoscopic devices (e.g., quantum dots and Aharonov-Bohm rings).

To accommodate fine-featured gates, one can grow shallow 2DEGs with depths as little as 15 nm at the expense of mobility.^{4–15} However, with such shallow heterostructures, one has to also contend with pronounced random telegraph signal (RTS) noise, or charge noise, associated with electrons hopping between dopant sites in the AlGaAs layer.¹⁶ Furthermore, the dopant layer may partially screen surface gates (through hopping conduction) and/or facilitate gate leakage. These effects are particularly detrimental to mesoscopic devices. Although one can perform a biased cooling^{17,18} or a thermal cure¹⁹ to attempt to drastically reduce the levels of charge noise on a given device, results from both techniques vary from device to device.

Both limitations described above can be circumvented by using undoped heterostructures in different geometries such as the semiconductor-insulator-semiconductor field-effect transistors^{20–24} (SISFET) or the heterostructure-insulator-gate field-effect transistors^{25–27} (HIGFET). Since there are no intentional dopants, the 2DEG can be brought much closer to the surface without sacrificing mobility. Furthermore, undoped quantum dots may also

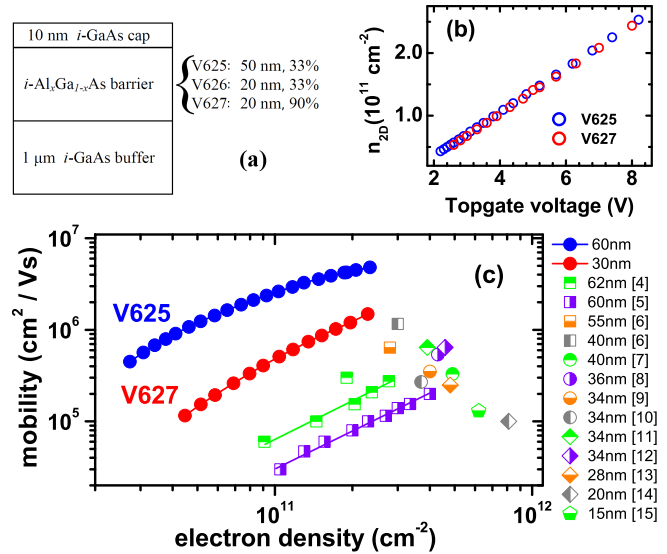


FIG. 1. (color online) (a) MBE layers used in our undoped heterostructures, with variations in AlGaAs barrier thickness (t) and Aluminium composition (x) for each undoped wafer used in this paper. A high Al content is required in the AlGaAs barrier for a stable ultra-shallow 2DEG to form (see text below). (b) Carrier density versus gate voltage for the V625 and V627 undoped 2DEGs. (c) Mobility versus electron density for undoped wafers V625 and V627, as well as various other doped wafers in shallow 2DEGs.^{4–15} Lines through data points indicate a gated measurement. The legend indicates the 2DEG depth below the surface.

interact with far fewer undesirable impurities in the vicinity than their doped counterparts. In this Letter, we compare ultra-shallow undoped and doped GaAs/AlGaAs 2DEGs, discuss the contributions of various scattering mechanisms, and demonstrate gated quantum dots on ultra-shallow undoped heterostructures.

Three undoped heterostructures were grown on the same day (V625, V626, and V627) with the MBE layers shown in Figure 1(a). The AlGaAs barrier thickness and Al composition x were varied systematically. Details of fabrication are otherwise identical to and extensively described in Ref. 28. The surface Ti/Au gates defining our quantum dots were fabricated by e-beam lithogra-

^{a)} Electronic mail: fs228@cam.ac.uk

phy directly on the surface of the GaAs cap, below the insulator layer (polyimide). Above the polyimide layer, a Ti/Au topgate covers the entire surface of the 2DEG and is used to vary the carrier density.

The typical failure mechanism in SISFETs and HIGFETs are electrical shorts between the ohmic contacts and the topgate.²⁹ None of our samples suffered from this problem. Indeed, the relationship between density and the topgate voltage is linear for V625 and V627 [Fig.1(b)], and the carrier density does not saturate with topgate voltage. Both observations are consistent with no leakage from the topgate to the 2DEG. However, we found that in V626 the AlGaAs barrier was not insulating enough to prevent charge leaking between the 2DEG and the semiconductor-insulator interface (a GaAs-polyimide interface in our case). Shortly after the 2DEG is fully induced, charge “seeps” through the AlGaAs barrier. As it gradually accumulates at the GaAs-polyimide interface, it begins to screen the topgate from the 2DEG, which results in a gradual loss of carriers until the 2DEG pinches off with time.³⁰ Increasing the energy height of the $\text{Al}_x\text{Ga}_{1-x}\text{As}$ barrier (by using $x = 0.90$ instead of $x = 0.33$) eliminated the “seeping” leak between the 2DEG and the GaAs-polyimide interface. The ultra-shallow 2DEG in V627 was stable in time and did not leak to the topgate, as do all our deeper undoped 2DEGs.

Figure 1(c) compares 2D transport characteristics between shallow GaAs/AlGaAs 2DEGs in our undoped wafers and a representative sample of published values of doped wafers. The large improvement in mobility (up to two orders of magnitude) is largely attributable to the absence of intentional dopants. Although scattering due to surface states is significant for a 2DEG depth less than 70 nm from the surface,²⁸ it is still by far the scattering from remote ionized impurities that impairs mobility in doped shallow 2DEG wafers.^{31,32} For 2DEGs much deeper than 70 nm, in undoped heterostructures, it may even be advantageous to avoid very deep 2DEGs, due to the reduced thickness of the relatively dirty AlGaAs barrier above the 2DEG (the background impurity concentration in $\text{Al}_{0.3}\text{Ga}_{0.7}\text{As}$ is about three times larger than in GaAs^{28,32}). For example, we have shown a slight improvement ($\sim 10\%$) in the mobility at the high-density limit of a 117nm deep 2DEG relative over a 317nm deep 2DEG in undoped heterostructures grown on the same day.³³ Lastly, we wish to emphasise that all undoped wafers are intrinsically gateable, unlike doped wafers. The ungateability of some doped wafers is not only restricted to shallow 2DEGs, but also can occur in high-mobility doped wafers.^{34–36}

It is only very recently that quantum dots have been successfully fabricated in undoped heterostructures with electrons³⁷ and holes.³⁸ No RTS event could be observed in the electron quantum dot fabricated on the SISFET of Ref. [37]. Figure 2 shows Coulomb blockade (CB) oscillations in the weak coupling regime from a quantum dot fabricated on HIGFET wafer V627. The plunger gate voltage is positive: the surface gates defining the

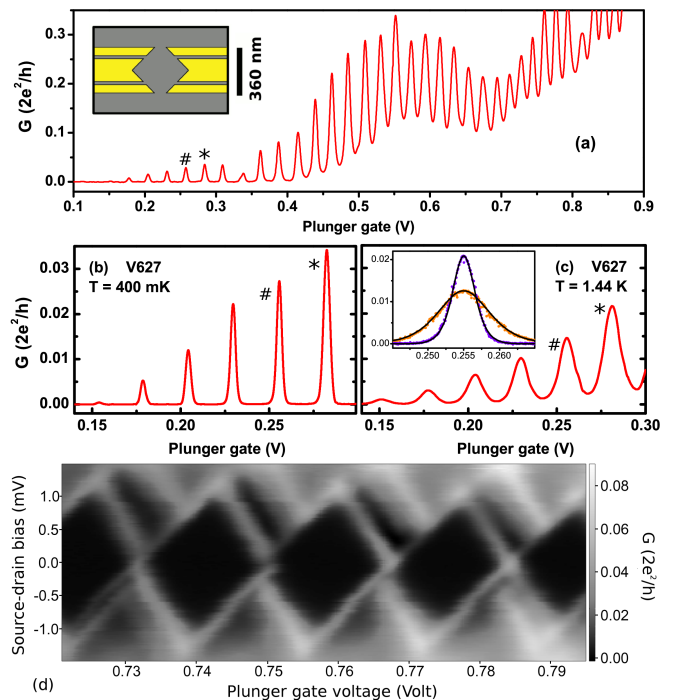


FIG. 2. (color online) (a) Measured differential conductance G (with $100 \mu\text{V}$ excitation) showing Coulomb blockade (CB) oscillations from a quantum dot defined with surface gates (see inset) on the HIGFET V627. All stated temperatures are electron temperatures, obtained from fits, and all CB data was obtained at a topgate voltage of 8.0V ($n = 2.5 \times 10^{11} \text{ cm}^{-2}$). The CB peaks marked with $*$ and $\#$ are further analyzed in Figure 3. (b) The dot is in the weak coupling regime. (c) Even at high temperature, the CB peaks are well resolved, indicative of a large charging energy. The inset shows two representative fits of the data to Eq. (1) for $T = 480 \text{ mK}$ and 1200 mK for CB peak $\#$. (d) Source-drain bias spectroscopy. The dot is in a slightly different regime than shown in panel (a). Parameters extracted from this data set are: the charging energy ($U = 1.25 \text{ meV}$), the single-particle energy level spacing ($\Delta E = 0.5 \text{ meV}$), the plunger gate lever arm ($\alpha = 0.083 \text{ meV/mV}$), the plunger capacitance ($C_g = e/\Delta V_g = 9.5 \text{ aF}$), and the total capacitance ($C_\Sigma = 128 \text{ aF}$).

quantum dot are partially screening the topgate and require a positive bias to help the topgate induce a 2DEG at the center of the quantum dot. Directly underneath the surface gates, the topgate is totally screened and a 2DEG does not form until a much higher positive voltage is applied to the surface gates. Effectively, there is a depletion radius extending beyond the lithographic dimensions of the surface gates, contributing to the smallness of the dot. This could make the lithography of ultra-small nanostructures much easier on undoped heterostructures than on doped wafers.

Despite its large dimensions [inset, Fig.2(a)], the charging energy ($U = e^2/C_\Sigma$, where C_Σ the total capacitance) of our quantum dot is rather large: $U = 1.25 \text{ meV}$ [Fig.2(d)]. By suitably changing gate voltages, U can be tuned as high as 1.75 meV , but the dot

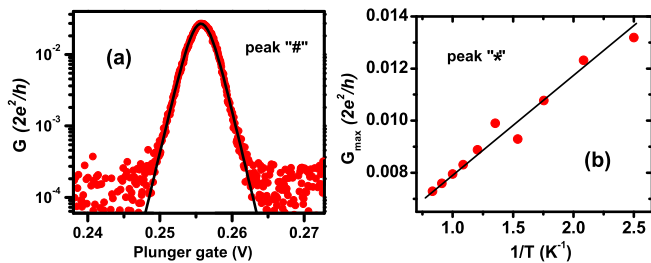


FIG. 3. (color online) Solid circles are the experimental data of the CB peaks in Fig. 2 labeled with: (a) # and (b) *. The solid lines are fits to Eqn. (1). Taken together, the data from both panels confirm single-particle energy levels only are involved in transport.

is then no longer in the weak coupling regime. The (weak coupling regime) charging energy in our HIGFET ($U = 1.25$ meV) is larger than that ($U = 0.5$ meV) of the quantum dot on the SISFET's from Ref. [37]. The single-particle energy level spacing (ΔE) of our quantum dot is also quite larger, $\Delta E \sim 0.50$ meV as opposed to $\Delta E \sim 0.05$ meV, and enables the observation of excited states at 400 mK. The total capacitance of our HIGFET dot (128 aF) is slightly less than that of the SISFET dot (160 aF), and is dominated by the capacitance to the large topgate above the quantum dot in both cases. Using the 2D electron density and the area implied by the measured total capacitance (assuming $C_\Sigma = \epsilon A/d$), there are at most ~ 80 electrons in our dot.

The energy scales of U and ΔE are directly related to the 2DEG depths of the SISFET (185 nm deep) and our HIGFET (30 nm deep). It is difficult to make shallow SISFET devices: the yield of working devices dramatically falls off with decreasing 2DEG depth, whereas it remains constant in HIGFET devices. Using $C_\Sigma = \epsilon A/d$ and the values above, we estimate a quantum dot fabricated on a hypothetical SISFET with a 30 nm deep 2DEG would have a large total capacitance, 800–1000 aF. It therefore appears more advantageous to fabricate quantum dots from HIGFETs rather than SISFETs.

Figure 3 and Figure 2(c) show fits to the equation:

$$G = \frac{e^2}{h} \frac{\Gamma_c}{kT} \cosh^{-2} \left[\frac{\alpha e(V_g - V_0)}{2kT} \right] \quad (1)$$

where Γ_c is a constant, α the lever arm of the plunger gate, and V_0 the plunger voltage at the center of the CB peak.³⁹ It describes the expected lineshape of CB peaks where transport only involves a single energy level. Theory fits our data well. Thus, the CB peaks shown in Fig. 2(b) are in the single-level transport regime $U \gg \Delta E \gg kT$.

In conclusion, we have shown ultra-shallow 2DEGs (within 30 nm of the surface) in undoped heterostructures that display no parallel conduction, are gateable, and show no hysteresis upon gate action. The absence of dopants has improved their mobility by up to two orders of magnitude relative to their doped counterparts with

similar 2DEG depths. We have also demonstrated that these undoped heterostructures can be used to fabricate single-electron quantum dots defined by surface metal gates, with charging energies of up to 1.75 meV and excited state energies of up to 0.5 meV.

The authors would like to thank S.J. Chorley and C.J.B. Ford for their help, and acknowledge financial support from Toshiba Research Europe and the EPSRC.

- ¹R. Dingle, H. L. Stormer, A. C. Gossard, and W. Wiegmann, *Appl. Phys. Lett.* **33**, 665 (1978)
- ²L. N. Pfeiffer and K. W. West, *Physica E* **20**, 57 (2003)
- ³V. Umansky, M. Heiblum, Y. Levinson, J. Smet, J. Nübler, and M. Dolev, *J. Cryst. Growth* **311**, 1658 (2009)
- ⁴G. Kopnov, V. Y. Umansky, H. Cohen, D. Shahar, and R. Naaman, *Phys. Rev. B* **81**, 045316 (2010)
- ⁵D. Laroche, S. Das Sarma, G. Gervais, M. P. Lilly, and J. L. Reno, *Appl. Phys. Lett.* **96**, 162112 (2010)
- ⁶A. J. M. Giesbers, U. Zeitler, M. I. Katsnelson, D. Reuter, A. D. Wieck, G. Biasiol, L. Sorba, and J. C. Maan, *Nature Phys.*, 364(2010)
- ⁷C. Rossler, B. Küng, S. Drüscher, T. Choi, T. Ihn, K. Ensslin, and M. Beck, *Appl. Phys. Lett.* **97**, 152109 (2010)
- ⁸R. Nemutudi, C.-T. Liang, M. J. Murphy, H. E. Beere, C. G. Smith, D. A. Ritchie, M. Pepper, and G. A. C. Jones, *Microelectronics Journal* **36**, 425 (2005)
- ⁹A. E. Gildemeister, T. Ihn, R. Schleser, K. Ensslin, D. C. Driscoll, and A. C. Gossard, *J. Appl. Phys.* **102**, 083703 (2007)
- ¹⁰S. Nakamura, Y. Yamauchi, M. Hashisaka, K. Chida, K. Kobayashi, T. Ono, R. Leturcq, K. Ensslin, K. Saito, Y. Utsumi, and A. C. Gossard, *Phys. Rev. Lett.* **104**, 080602 (2010)
- ¹¹A. Mühle, W. Wegscheider, and R. J. Haug, *Appl. Phys. Lett.* **92**, 013126 (2008)
- ¹²C. Fricke, F. Hohls, W. Wegscheider, and R. J. Haug, *Phys. Rev. B* **76**, 155307 (2007)
- ¹³R. Nemutudi, M. Kataoka, C. J. B. Ford, N. J. Appleyard, M. Pepper, D. A. Ritchie, and G. A. C. Jones, *J. Appl. Phys.* **95**, 2557 (2004)
- ¹⁴D. Goldhaber-Gordon, H. Shtrikman, D. Mahalu, D. Abusch-Magder, U. Meirav, and M. A. Kastner, *Nature* **391**, 156 (1998)
- ¹⁵D. J. Goldhaber-Gordon, Ph.D. thesis, M.I.T. (1999)
- ¹⁶Y. Li, C. Ren, P. Xiong, S. von Molnar, Y. Ohno, and H. Ohno, *Phys. Rev. Lett.* **93**, 246602 (2004)
- ¹⁷M. Piore-Ladriere, J. H. Davies, A. R. Long, A. S. Sachrajda, L. Gaudreau, P. Zawadzki, J. Lapointe, J. Gupta, Z. Wasilewski, and S. Studenikin, *Phys. Rev. B* **72**, 115331 (2005)
- ¹⁸C. Buizert, F. H. L. Koppens, M. Piore-Ladriere, H. P. Tranitz, I. T. Vink, S. Tarucha, W. Wegscheider, and L. M. K. Vandersypen, *Phys. Rev. Lett.* **101**, 226603 (2008)
- ¹⁹M. Fujiwara, M. Sasaki, and M. Akiba, *Appl. Phys. Lett.* **80**, 1844 (2002)
- ²⁰B. E. Kane, L. N. Pfeiffer, K. W. West, and C. K. Harnett, *Appl. Phys. Lett.* **63**, 2132 (1993)
- ²¹J. Herfort and Y. Hirayama, *Appl. Phys. Lett.* **69**, 3360 (1996)
- ²²A. Kawaharazuka, T. Saku, C. A. Kikuchi, Y. Horikoshi, and Y. Hirayama, *Phys. Rev. B* **63**, 245309 (2001)
- ²³D. J. Reilly, T. M. Buehler, J. L. O'Brien, A. R. Hamilton, A. S. Dzurak, R. G. Clark, B. E. Kane, L. N. Pfeiffer, and K. W. West, *Phys. Rev. Lett.* **89**, 246801 (2002)
- ²⁴M. P. Lilly, J. L. Reno, J. A. Simmons, I. B. Spielman, J. P. Eisenstein, L. N. Pfeiffer, and K. W. West, *Phys. Rev. Lett.* **90**, 056806 (2003)
- ²⁵R. H. Harrell, K. S. Pyshkin, M. Y. Simmons, D. A. Ritchie, C. J. B. Ford, G. A. C. Jones, and M. Pepper, *Appl. Phys. Lett.* **74**, 2328 (1999)
- ²⁶H. Noh, M. P. Lilly, D. C. Tsui, J. A. Simmons, E. H. Hwang, S. Das Sarma, L. N. Pfeiffer, and K. W. West, *Phys. Rev. B* **68**, 165308 (2003)

- ²⁷R. L. Willett, L. N. Pfeiffer, and K. W. West, *Appl. Phys. Lett.* **89**, 242107 (2006)
- ²⁸W. Y. Mak, K. D. Gupta, H. E. Beere, I. Farrer, F. Sfigakis, and D. A. Ritchie, *Appl. Phys. Lett.* **97**, 242107 (2010)
- ²⁹S. Sarkozy, K. D. Gupta, F. Sfigakis, I. Farrer, H. E. Beere, R. Harrell, D. A. Ritchie, and G. A. C. Jones, *Electrochemical Soc Proc.* **11**, 75 (2007)
- ³⁰The timescale for this process is of order of a several minutes, with factors being the resistance and capacitance across the Al-GaAs barrier (thus determining an RC time constant), and the speed at which the topgate is ramped (or if held steady). In this scenario, we emphasize that no leakage is observed between the 2DEG and the topgate: no current flows through the insulating polyimide layer beneath the metallic topgate.
- ³¹A. Gold, *Phys. Rev. B* **38**, 10798 (1988)
- ³²S. J. MacLeod, K. Chan, T. P. Martin, A. R. Hamilton, A. See, A. P. Micolich, M. Aagesen, and P. E. Lindelof, *Phys. Rev. B* **80**, 035310 (2009)
- ³³F. Sfigakis, K. D. Gupta, S. Sarkozy, I. Farrer, D. A. Ritchie, M. Pepper, and G. A. C. Jones, *Physica E* **42**, 1200 (2010)
- ³⁴J. B. Miller, I. P. Radu, D. M. Zumbuhl, E. M. Levenson-Falk, M. A. Kastner, C. M. Marcus, L. N. Pfeiffer, and K. W. West, *Nature Phys.* **3**, 561 (2007)
- ³⁵M. Dolev, M. Heiblum, V. Umansky, A. Stern, and D. Mahalu, *Nature* **452**, 829 (2008)
- ³⁶C. Rossler, T. Feil, P. Mensch, T. Ihn, K. Ensslin, D. Schuh, and W. Wegscheider, *New J. Phys.* **12**, 043007 (2010)
- ³⁷A. M. See, O. Klochan, A. R. Hamilton, A. P. Micolich, M. Aagesen, and P. E. Lindelof, *Appl. Phys. Lett.* **96**, 112104 (2010)
- ³⁸O. Klochan, J. C. H. Chen, A. P. Micolich, A. R. Hamilton, K. Muraki, and Y. Hirayama, *Appl. Phys. Lett.* **96**, 092103 (2010)
- ³⁹E. B. Foxman, P. L. McEuen, U. Meirav, N. S. Wingreen, Y. Meir, P. A. Belk, N. R. Belk, M. A. Kastner, and S. J. Wind, *Phys. Rev. B* **47**, 10020 (1993)